

OECF characterization of a non-linear HDR Color Camera for Automotive Applications

Dirk W. Hertel, Edward Chang; Sensata Technologies, Inc.; Cambridge, MA/USA

Abstract

Video cameras used in automotive applications such as driver assistance systems are confronted with natural scenes where light levels vary widely, and the luminance range within scenes can also be extremely wide. Only sensors that capture the full dynamic range of natural scenes in a single frame with sufficient image quality performance and at low cost are suitable for automotive applications. This is accomplished by CMOS technologies that extend the pixel's dynamic range by non-linear highlight compression, but can then cause scene dependent color balance errors to appear in certain scene elements.

In silver-halide color reversal films, color balance is maintained over a wide dynamic range by tightly controlling the tone reproduction curves in each color channel. Color correction in a non-linear HDR camera requires the knowledge of its tone reproduction curves. We adapted the ISO 15739 test chart method to HDR requirements to realize its potential to provide a one-step measurement which would characterize the entire image capture system including optics and image processing as well as realistic photospace conditions. This paper reports initial OECF and color balance data from a direct non-linear HDR color camera for automotive applications.

Introduction

Camera-based driver assistance systems are increasingly used in the automotive industry [1]. Although monochrome cameras still dominate, the value of color information gains increasing recognition. Applications range from visual assistance systems where forward and rearview images are displayed on a dashboard screen to active safety systems where the video footage is analyzed by software. Automotive cameras must work under an extremely wide range of scene conditions: not only do the light levels change between day, night, outdoor and indoor conditions (tunnels, parking garages), but also the luminance range *within* the scene can be extremely high, especially when light sources such as the sun or headlights are located within the frame. Apart from being required to capture natural scenes with a high luminance ratio, automotive cameras need frame rates that are sufficiently high for video applications, a sensitivity that is sufficiently high for night vision applications, a signal-to-noise ratio that is sufficiently high for reliably running machine vision applications, and low cost. Automotive color cameras are required to differentiate between signal colors and reproduce them so that they are reliably recognizable by the human observer or machine vision algorithms. This task is often difficult at night when color signals such as traffic lights constitute the peak luminance levels of the scene so that pixel saturation can severely desaturate the signal colors and make recognition and differentiation awkward.

Without adjusting its pupil or allowing time for adaptation, the human eye can only capture a luminance range of less than 40dB at a time. However while scanning natural scenes the eye adapts to different light levels so that a much higher range of more than 90dB can be captured *sequentially* [2]. This observation led to the idea of capturing large luminance ranges by a sequence of images taken at different exposures, and it was first practiced with film, reaching 160dB [3], then later with digital cameras [4]. Although sequential multi-exposure techniques with linear image sensors allow tight control of tone and color reproduction as well as the removal of lens flare, their applicability for automotive video is limited by frame rate, sensitivity and the need for costly frame buffers. Parallel multi-exposure techniques using arrays of linear imagers or groups of pixels within a linear imager are too expensive for automotive applications [5].

Automotive applications are best suited by imagers that capture the high scene luminance range *simultaneously* within each frame, and map the scene luminance to an 8-bit space so that it can be output to low-cost processing and display devices. Such direct capture of HDR imagery requires the response curve of the image sensor to cover the luminance range of the natural scene [6]. According to ISO 14524 the relationship between input scene log luminances (units: \log_{10} cd/m²) and digital output levels is described by the Opto-Electronic Conversion Function OECF [7]. However, less than the entire luminance range covered by the OECF is usable for reliably capturing image information. A luminance signal can be recorded reliably only where the incremental signal-to-noise ratio (iSNR), the ratio of the incremental output signal to the rms noise level at a particular signal level, exceeds a minimum threshold. ISO 15739 specifies a threshold of one [8]. iSNR drops below this threshold at very low luminance levels where the slope of the OECF is low and noise is high, and very high luminance levels where saturation sets in. The ratio between these two levels is the ISO dynamic range (DR, in units of dB), a measure of the luminance range that is usable for reliably capturing scene information.

Direct HDR technologies extend the dynamic range by delaying the saturation at high luminance levels. Autobrite® technology achieves this by introducing multiple barriers of variable height that repeatedly reset the CMOS pixel during integration time if the peak luminance exceeds the sensor's linear range [9], [10]. By means of variable height/multiple reset barriers a wide range of response curves can be achieved, ranging from linear response in low light to various degrees of non-linear response in bright light. The principle is illustrated in Fig. 1 for a single barrier. The nonlinear response curve is approximated by a series of piecewise linear sections with increasing compression (multiple slopes). The total integration time and dynamic range extension are governed by two feedback loops that analyze image statistics: the exposure control loop uses the mean brightness to

adjust the total exposure time. The compression control loop deploys the barriers in order to ensure that no pixels are saturated whilst the image fills the whole histogram.

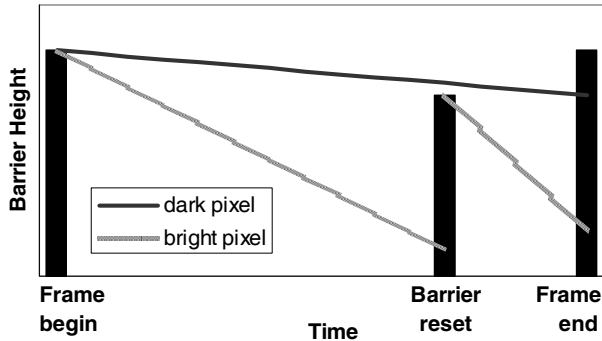


Figure 1. Autobrite pixel with single barrier: barrier reset prevents the bright pixel from saturating, but has no effect on dark pixel.

The application to color requires decompression to convert the signal taken in Autobrite mode into an equivalent linear signal. The decompression curve can be calculated from the piecewise linear response curve so that good color reproduction can be expected. However, several factors such as timing quantization, variation in barrier height, non-linearity of the pixel response and rounding near the barrier breakpoints can cause variations so that the actual response curves of the imager do not exactly match the decompression curve. This leads to color casts that can change magnitude and direction across the tonescale, for example ‘pink clouds’ due to imbalance in the highlight regions. The exact knowledge of the effective OECF is necessary to develop strategies for correcting these color errors.

This paper explores available methods to measure the OECF of a non-linear HDR color video camera for automotive applications. Metrics for estimating the visual impact of color balance errors are applied to OECF data in linear and HDR modes.

Experimental

Automotive Photospace

The performance of an image capture system is not only limited by its lens, imager and image signal processing, but also by the external image-taking conditions such as scene illuminance and camera-object distance which can vary widely. These factors, also referred to as “photospace”, lie beyond the control of the system designer but they substantially influence the performance of the imaging system [11] and thus determine the yield of images that are usable for the intended purpose of detecting image information.

The photospace distribution $PSD(L, d)$ is the statistical description of the frequency of image capture as a function of the primary photospace coordinates object luminance level L and camera-object distance d . Photospace information can be used as a design tool to maximize the image quality for the intended usage conditions [11].

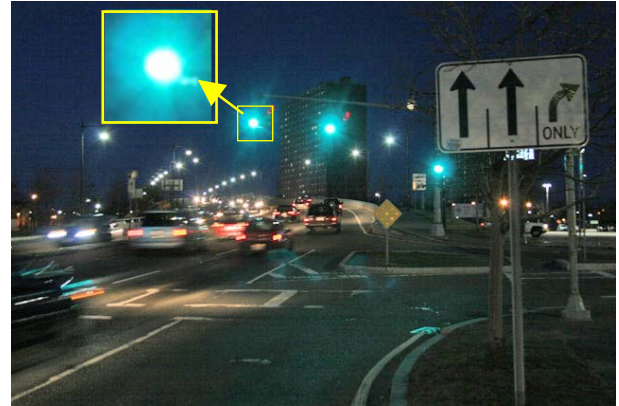


Figure 2. Typical high-dynamic range night scene where the highlights are saturated and thus colorless (insert shows enlarged traffic signal).

The dynamic range of a natural scene is not determined by its overall brightness but by the luminance *ratio* between the brightest highlight and the deepest shadow. A dazzling sunlit scene might be perceived as ‘high dynamic range’, yet luminance measurements of the scene elements using a spot meter showed that its luminance range can be as low as 10:1. High dynamic range scenes occur in situations where light sources are imaged directly or as reflections (spotlights), and deep shadows are present (including night scenes), since the luminance range within the scene is determined by the luminance ratio of the brightest spotlight and that of the deepest shadow. The amount of light reflected by surfaces depends on weather conditions, for example damp road surfaces reflect only about half the light of dry ones. Fig. 2 shows a typical night traffic scene. A digital spot meter (1°) was used on-site to measure the luminance levels of important scene elements, and the scene content was documented with a digital camera. Traffic signals and headlights determine the peak luminance level, and road surfaces the lowest. The estimated luminance range of the scene in Fig. 2 was 8,000 : 1, which would require a camera with a dynamic range of at least 80dB. The actual luminance range is expected to be higher because of lens flare in the spot meter, but the estimate is still valid because lens flare occurs to an even higher degree in typical automotive cameras. The camera used to document the scene (Fig. 2) had a dynamic range of less than 80dB; the color of the traffic signal is only revealed by the aura caused by lens flare; the pixels within the actual lights are saturated and thus appear colorless.

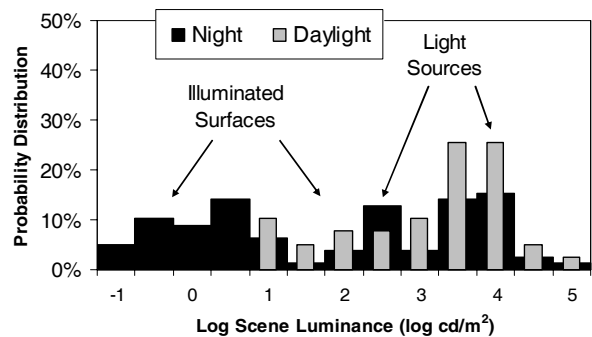


Figure 3. Initial automotive photospace data with clusters for light sources and illuminated surfaces [12].

Fig. 3 shows photospace distributions $PSD(L)$ from on-site measurements within 12 automotive daytime and night scenes. The distributions show clusters representing light sources (reflections of sun, vehicle lights, street lights, traffic lights) at high luminance levels, with illuminated surfaces (road surface, traffic signs and traffic participants) at the low luminance end of the distributions. The distributions show that the luminance ratio within night scenes (10^6) can be expected to be higher than that of daylight scenes (10^4 - 10^5), due to the much lower luminance of illuminated objects at night.

Objective image quality measurements

In order to estimate the ability of a digital camera to capture tonal and color detail, two functions must be measured: the levels of digital output values (OECF) and the levels of noise corresponding to defined levels of input exposure. Full characterization would also require MTF [13]. These characteristics are measured separately for each color channel of a color camera. Originally defined for photographic films, this methodology has been successfully applied to digital imaging systems, and forms the basis of ISO standards for characterizing digital camera image quality. The usefulness of this methodology to characterize non-linear color cameras will be explored in this initial study.

ISO-standard based OECF and noise measurements

ISO 14524 [7] describes the OECF measurement for digital cameras. It is complemented by ISO 15739 [8] combining OECF with noise measurements. Both standards suggest two alternative methods for measuring OECF and noise: focal plane (lens removed) and whole camera.

- The focal plane method captures the range of input illuminance levels *sequentially* in a series of different uniform exposures, ranging from the noise limit of sensitivity to saturation. There is no physical limit to the luminance range. Parameters calculated from focal-plane measurements estimate the *capability* of the image sensor, for example dynamic range.
- The camera method uses a test chart to modulate the input illuminance levels, and captures them *simultaneously* in a single exposure. The camera OECF test charts simulate a scene with a specific luminance ratio and average luminance distribution [7]. Although the luminance distribution of real-world scenes may significantly differ from that of the test chart, these OECFs represent the effective sensitivity curves [14], including the effects of lens, flare, image sensor, and processing algorithms.

Thus the test-chart method is closer to imaging real-world scenes than the focal plane method and thus evaluates the *performance* of the camera as a whole imaging system.

A limitation of the test-chart OECF method is the luminance range that can be produced simultaneously from a physical test chart since conventional standard reflection test charts only cover contrast ranges up to 160:1. Fig. 4 shows the recently developed transmission test chart with 20 test patches simultaneously covering a luminance range of $5 \cdot 10^4$. When this is combined with an integrating sphere illuminator where the peak luminance levels can be adjusted over a range of 10^4 [15], an overall luminance range of over 10^8 can be covered in a series of exposures.

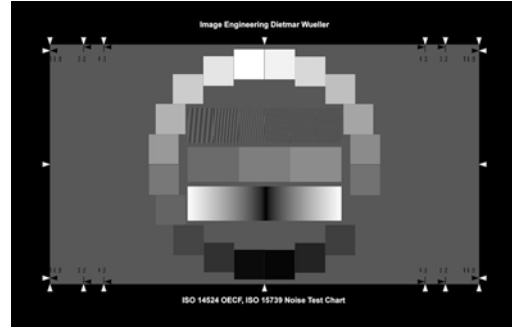


Figure 4. Transmission test chart for combined measurement of OECF (ISO 14524) and noise (ISO 15739) [15].

The controlled variation of the peak illuminance level is essential for characterizing the adaptive non-linear dynamic range extension because the automatic adaptation is activated by two parameters: mean luminance governing integration time, and peak luminance governing the amount of HDR extension. The controlled variation of the peak luminance level is also essential for simulating photospace conditions over a wide range of scene luminance levels

Comparing focal plane and test-chart OECF

Fig. 5 shows a comparison of focal plane and test-chart OECFs for a camera with an Autobrite [10] HDR monochrome VGA sensor. A logarithmic abscissa as recommended by ISO 14524 [7] and ISO 15739 [8] is used to accommodate the total luminance range of 120dB. The two different modes of linear and HDR operation were triggered by changing the luminance levels of the test illuminators. At low luminance levels with a peak luminance of 11 cd/m^2 , typical for illuminated surfaces in night scenes such as Fig. 2, the exposure control maximized the integration time. The compression control left the sensor in linear mode which was sufficient to image all luminance levels without clipping. When the luminance level was increased by a factor of 100, the control loops reduced the integration time to maintain average image brightness, and activated the barriers of the HDR highlight compression to avoid clipping.

Veiling glare distorted the test-chart OECFs by increasing the camera digits at the dark end of the OECF. The effect depends on lens and scene (test chart), and here it increased from 0.6% at low light to 8% at the bright setting. This made comparison with the flare-free focal plane measurements difficult, but after normalizing the test chart OECFs and the focal plane data agreed very well (see Fig. 5), demonstrating the utility of the transmission test chart method for HDR image quality evaluation.

Fig. 6 shows the incremental signal-to-noise ratios (iSNR) calculated from the test-chart OECF of Fig. 5, and noise measurements [8]. The luminance range usable for the capture of image information stretches from the lowest luminance where iSNR meets a threshold of one to the peak luminance levels of the test chart. The adaptation of the Autobrite response curves effectively prevents the loss of highlight information due to clipping. The ISO dynamic range of 56dB in linear mode increases to 71dB in HDR mode.

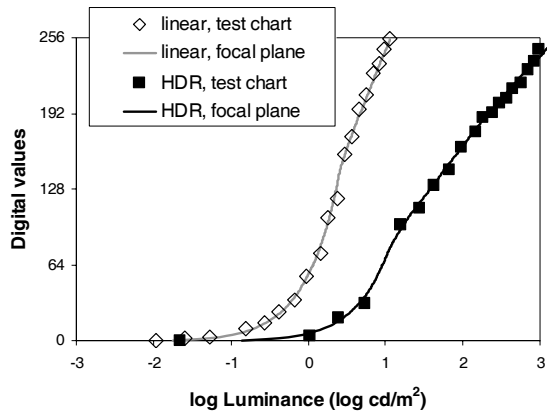


Figure 5. Comparison of OECF measurements on a monochrome Autobrite camera: focal plane (lines) vs. test-chart (points) at linear and HDR mode.

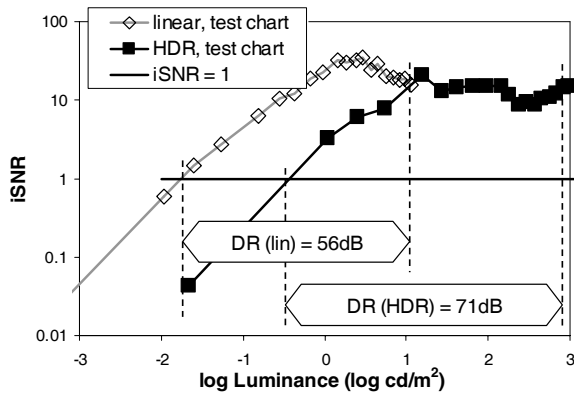


Figure 6: Incremental signal-to-noise ratio (ISO 15739) of an Autobrite monochrome camera in linear and HDR mode.

OECFs of a color HDR camera

Fig. 7 shows the OECFs for a color camera in linear and HDR mode. As for the monochrome camera, the different modes of linear and HDR operation were triggered by changing the peak luminance level of the test chart illuminator. In linear mode the OECFs of the three color channels agree very well, delivering images with excellent neutrality. However, in HDR mode color casts occur in some of the test patches, and the OECFs show considerable differences between the color channels that change with luminance. The crossover points between the red, green and blue OECFs indicate that the color balance error changes magnitude and direction across the luminance range where the HDR extension is active. The color errors indicate a mismatch between the decompression curves used for color processing, and the actual pixel response curves. The mismatch is mainly due to quantization in barrier timing, and die-to-die variation of barrier height.

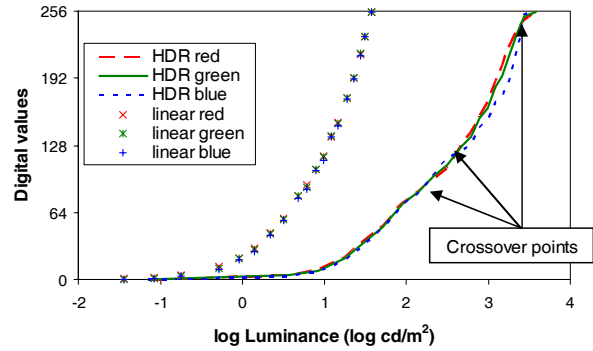


Figure 7. Equalized OECFs of the three color channels of an Autobrite color camera in linear (points) and HDR mode (lines).

Image quality metrics

Direct comparison of such characteristic functions as OECF does not necessarily predict differences in image quality performance. These comparisons require application-specific metrics calculated from the characteristic functions, for example metrics that describe the perception of color image attributes by a human observer [16]. An example of a metric that evaluate the detection of color information by machine-vision algorithms is the discriminability of signal colors [17]. If the signal colors fall into the saturation region of the OECF, then luminance and chrominance ratios are diminished to a degree that the signals are no longer discriminable.

Estimating color balance in a human visual application

An example of a human vision application is a driver assistance system where the color image from a rearview camera is displayed on a dashboard monitor. In order to estimate the visibility of color balance errors, the RGB image data were converted into CIELAB color space, and deviations from neutral in units of Δa^* , Δb^* , and ΔC^* were calculated (Figs. 8 and 9).

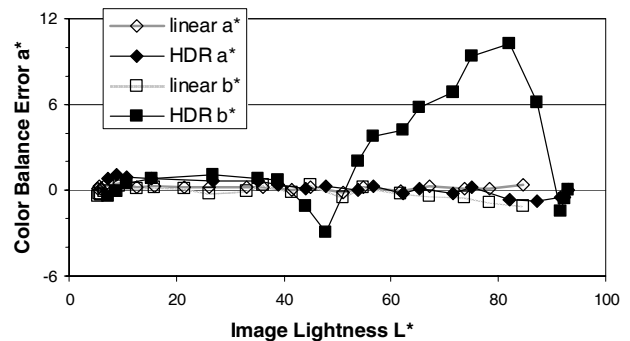


Figure 8. CIELAB Δa^* and Δb^* color balance errors vs. image lightness L^* in the OECF test images of Fig. 7 taken in linear and HDR mode.

Fig. 8 shows that the largest color balance error occurs in the b^* channel in HDR mode. As already indicated by the OECF curves, the color cast changes from a slight bluish tinge in the

midtones to a strong yellow cast in the highlights (55 to 90L*). Local color balance algorithms would be required for correction.

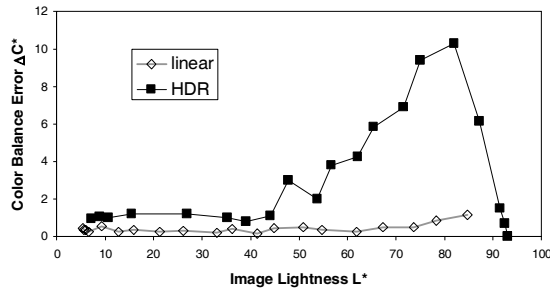


Figure 9. CIELAB ΔC^* color balance error vs. image lightness L^* in the OECF test images of Fig. 7.

The total color balance error in units of ΔC^* vs. L^* is shown in Fig. 9. It stays below 1 in linear mode, but reaches up to 12 in HDR mode, occurring mainly in the midtones and highlights (40 – 90L*). Although color balance shifts of this magnitude are clearly visible, for example as yellowish tarmac, it is still to be determined in psychovisual experiments whether they will impede the application of HDR color in a rearview driver assistance system.

Conclusions

OECFs of a digital camera with non-linear HDR extension were compared in linear and non-linear HDR mode. Excellent agreement was found for focal plane and camera measurements using high-contrast transmission test charts.

The deviations between the three color channels in the non-linear HDR extension of the OECF were quantified, and color balance errors estimated for a human visual application. Future work will concentrate on designing local color balancing algorithms based on the data collected from the OECF measurements, and on developing performance metrics for machine vision applications.

References

[1] Technical White Paper: Automotive Cameras for Safety and Convenience Applications, Sensata Technologies, <http://www.sensata.com/products/sensors/auto-whitepapers.htm>

[2] R. W. G. Hunt, The Reproduction of Colour. West Sussex, England: John Wiley and Sons (2004).

[3] C. W. Wyckoff, S. A. Feigenbaum, An Experimental Extended Exposure Response Film, SPIE, 1, 117 (1963).

[4] S. Mann, R. W. Picard, On being 'undigital' with digital cameras: Extending Dynamic Range by Combining Differently Exposed Pictures, Proc. IS&T's 48th Annual Conference, pg 422. (1995).

[5] R. Hicks, V. Raghavan, CMOS-Kamera mit grossem Dynamikbereich (CMOS camera with wide dynamic range), elektronik industrie 5, 74 (2006).

[6] E. Reinhard, G. Ward, S. Pattanaik, P. Debevec, High Dynamic Range Imaging. San Francisco: Morgan Kaufmann 2006, ch. 2, 4.

[7] Photography — Electronic still-picture cameras — Methods for measuring opto-electronic conversion functions (OECFs), ISO Standard 14524:1999(E).

[8] Photography — Electronic still-picture imaging — Noise measurements, ISO Standard 15739:2003(E).

[9] S. Decker, R.D. McGrath, K. Brehmer, C.G. Sodini, A 256 x 256 CMOS Imaging Array with Wide Dynamic Range Pixels and Column-Parallel Digital Output, IEEE J. Solid-State Circuits, vol. SC-33, No. 12, pg. 2081 (1998).

[10] Technical White Paper: Autobrite® Imaging Technology, Sensata Technologies, <http://www.sensata.com/products/sensors/auto-whitepapers.htm>

[11] B. W. Keelan, Handbook of Image Quality. New York: Dekker, 2002, ch. 27.

[12] D. Hertel, E. Chang, Image Quality Standards in Automotive Vision Applications, Proc. IEEE Intelligent Vehicles '07, pg. 404 (2007).

[13] E. Görgens, Objective evaluation of image quality, J. Inf. Rec. Mater. 15, pg. 305 (1987).

[14] D. Williams, "Debunking Specsmanship: Progress on ISO/TC42 Standards for Digital Capture Imaging Performance," Proc. IS&T PICS, pg.77 (2003).

[15] D. Wueller, "Evaluating digital cameras," in Proc. SPIE-IS&T Electronic Imaging, 2006, SPIE vol. 6069, 60690 K1-15.

[16] D. Hertel, E. Chang, L. Shih, J. Sproul, "Performance evaluation of digital still camera image processing pipelines," in Proc. SPIE-IS&T Electronic Imaging, 2007, SPIE vol. 6494, 64940 A1-12.

[17] F. Kimura, T. Takahashi, Y. Mekada, I. Ide, H. Murase, T. Miyahara, Y. Tamatsu, Measurement of Visibility Conditions toward Smart Driver Assistance for Traffic Signals, Proc. IEEE Intelligent Vehicles '07, pg. 636 (2007).

Author Biography

Dirk Hertel received his degree in physics (1979), and Ph.D. (1989) for imaging research from the Technical University Dresden (Germany), where he then worked as assistant lecturer in imaging science. From 1998 he worked at Polaroid on photo print quality optimization, and from 2005 at Cypress Semiconductor on image quality evaluation of digital cameras for mobile applications. Since 2007 he has been with Sensata, developing image quality metrics and models for automotive high dynamic range cameras. He participates in the I3A CPIQ Initiative and is a member of the IS&T, the German Society for Photography (DGPh), and the Colour Group (Great Britain).